

Stable information transfer network facilitates the emergence of collective behavior of bird flocks

Jiaping Ren¹, Wanxuan Sun¹, Dinesh Manocha², Aming Li³
and Xiaogang Jin¹

¹ State Key Lab of CAD&CG, Zhejiang University, Hangzhou 310058, China

² Department of Computer Science, University of North Carolina at Chapel Hill, Chapel Hill, North Carolina, USA

³ Chair of Systems Design, ETH Zurich, Weinbergstrasse 56/58, Zurich CH-8092, Switzerland

E-mail: jin@cad.zju.edu.cn

Abstract. Collective behavior is ubiquitous in living systems, ranging from human crowds to microbial communities, insect swarms, and bird flocks. It is widely reported that simple temporal local interactions between individuals may lead to the emergence of collective behavior. However, it is hard for dynamical models with time-varying neighborhoods to achieve coherent behaviors for large-scale flocks, and interactions are normally not instantaneous. Here, we build an information transfer network where interactions last for a certain period of time, and then combine this with a dynamical model of self-propelled particles. We find that the model with stable information transfer network creates a bird flock with a more realistic and robust performance. We further show that the time of information transfer in a flock grows logarithmically with its size and is proportional to the average response time of birds. Moreover, we find that the ranking curves displaying the order that birds first perceive an external stimulus are similar in shape for different flocks. Our results demonstrate that, beyond the traditional temporal local interactions, the stable information transfer network serves as an efficient mechanism for the emergence of large-scale collective behavior.

Keywords: collective intelligence, flocking, communication networks

1. Introduction

Collective behavior of individuals in large groups is widespread in nature, and occurs in various species [1], such as bacteria, midges, fish, birds, human beings, etc [2, 3, 4, 5, 6]. Various theories of collective behavior have been developed in many fields, including ecology [7], biology [8], physics [9, 10], computer science [11], economics [12], control theory [13, 14], and social science [15, 16, 17]. As a unit, aggregations often outperform simple sums of individuals [18]. For example, bird flocks escape from predators with a higher probability of success, honey bee swarms have the ability to find or build a comb, and bacteria colonies reverse their directions to expand rapidly [19, 20, 21]. But, how do animals coordinate with each other to achieve such adaptive collective behaviors?

With simple rules of local interaction, many collective behaviors among groups can be modeled [22, 23, 24, 25, 26, 27, 28, 29]. However, the mechanism for the global information transfer through this kind of local interaction remains a mystery. Marginal opacity was introduced to represent long-range information exchange [30], but this method becomes invalid for flocks with thousands of birds. Recently, scientists believe that an individual bird interacts with six to seven birds on average, rather than interacts with all birds within a certain Euclidean distance [31, 5]. These models and empirical observations suppose that birds interact with nearest birds, and thus neighborhood of each bird varies over time. But Coherent Neighbor Invariance theory states that the neighborships among individuals tends to be invariant in coherent behaviors [32]. Besides, it has been shown that equilibrium inference with fixed interaction network can produce consistent results with dynamical inference by analyzing the data from flocking events with 50 to 600 individuals [33]. Therefore, the fundamental mechanism favoring the emergence of collective behavior remains elusive.

In this work, we employ graph theory [34] to model the information transfer network of bird flocks. Within this stable information transfer network, each bird only transfers information with fixed neighbors, and information received by one bird can be transferred to an arbitrary bird in the same flock. We analyze information transfer time by changing the flock size, response time, number of reaction birds and time unit. The results show that information transfer time grows logarithmically with the size of flock, increases linearly with response time, scarcely decreases with number of reaction birds and is irrelevant to time step after error being eliminated. We also explore the process of information transfer through the flock. We find that the ranking curves displaying the order that birds first perceive an external stimulus with response time obeying a Gaussian distribution are closer to the real world, and they are similar in shape for different flocks. We further compare our stable information transfer network with traditional unstable information transfer network by analyzing the process of information transfer, polarization, correlation and average distance. Our experiments demonstrate that stable local interactions lead to more realistic and robust collective behavior especially for flocks with large scale.

2. Stable information transfer network: an invariant graph

We construct a directed three-dimensional (3D) graph $G = (V, E)$ (Fig. 1A) to model the stable information transfer network of a bird flock, where V and E represent the set of nodes and edges, respectively. We take the bird i in the flock as node $i \in V$ in G , and define Ω_i as the set of nodes which represent birds that have connections with node i . The number of nodes in V is N . E_i denotes the set of directed edges ending at i and starting from i 's neighbors, i.e., $E_i = \{e_{ji} | j \in \Omega_i\}$. The indegree of each node i is $d_{\text{in}}(i) = 6$, i.e., each bird only connects with six birds. Within this information transfer network, birds only perceive information from the neighbors connected to them.

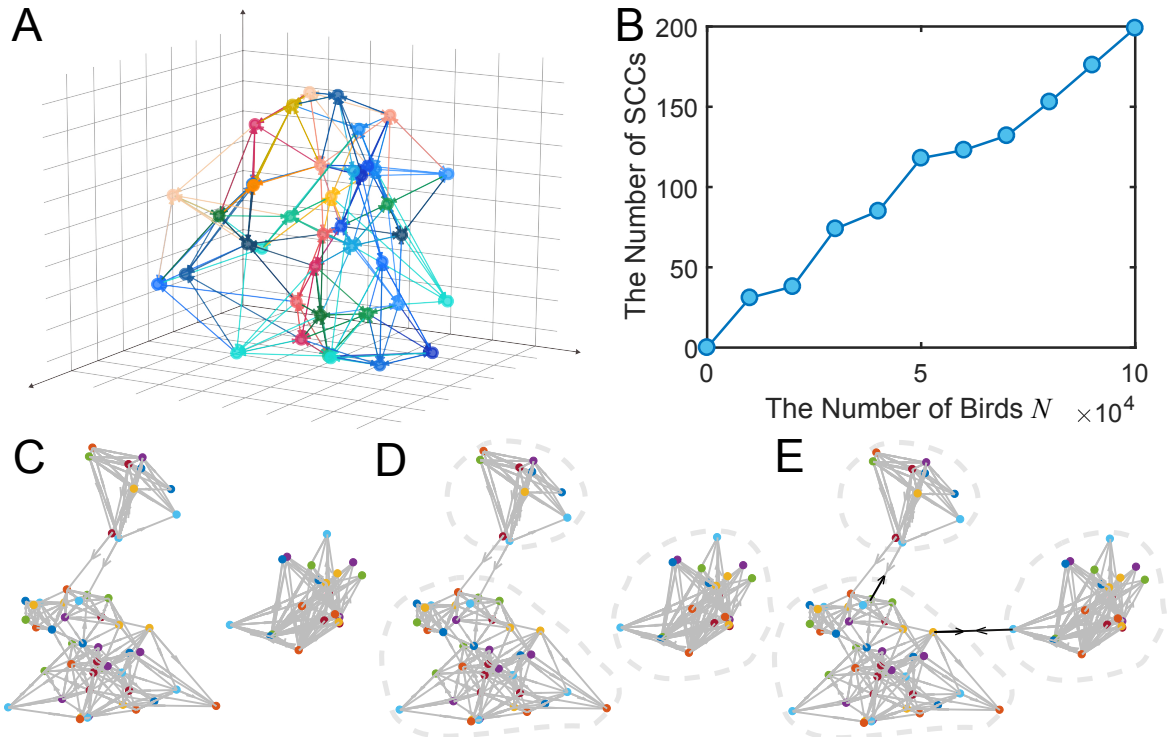


Figure 1. (A) The invariant directed graph in 3D. Each node represents a bird in the flock, and is adjacent to the six edges ended by it. If there are two arrows on one edge, the two nodes adjacent to this edge can propagate information with each other. (B) The number of strongly connected components (SCCs) with different numbers of birds in a flock (the number of birds ranges from 0 to 100,000). The nodes in each SCC can transfer information. (C) The 3D graph G describing the connections between birds (with 70 birds in total). For illustration, G contains three typical kinds of SCCs: sink, source and isolated component, and each only has one. (D) We compute the strongly connected components of the graph shown in (C). Each component is distinguished from the others with a closed, dashed gray circle. (E) We add a minimum number of edges (black arrows) to make G strongly connected.

For node i in graph G , we randomly assign it a 3D position and find the six nearest nodes as its neighbors. With the development of the whole flock's locomotion, these neighbors are not always nearest to it. In order to explore the strong connectivity

of G , we use the Eswaran-Tarjan algorithm [34] to find all of its strongly connected components (SCCs) in which every node is reachable from other nodes. G is a strongly connected graph if it only has one SCC. In our experiments, we test 0 to 100,000 birds forming a flock. The number of strongly connected components corresponding to the number of birds in one flock is shown in Fig. 1B. With more birds, the number of strongly connected components of G is larger, and G is farther from being a strongly connected graph. This indicates that information first obtained by a certain bird may not be propagated to all of the other birds in the same flock, and this is not consistent with scale-free spatial correlation theory [35]. In addition, the birds that are not fully connected to other birds cannot receive important information, such as danger signals, in time to react. As a result, a strongly connected graph is needed to model the information transfer between the birds.

Taking the set of nodes V as input, we first add edges e_{ji} for each node i with their six nearest neighbors $j \in \Omega_i$, and then add edges to make G (Fig. 1C) strongly connected. To simplify the graph G , we find strongly connected components (SCCs) for G , and condensing G to a directed acyclic graph G^* , thus get sources (with indegree zero), sinks (with outdegree zero), and isolated nodes (with both indegree and outdegree zero) of G^* (Fig. 1D). The nodes of G^* correspond to the strongly connected components of G .

Let s_1, s_2, \dots, s_p be sources in G^* , and w_1, w_2, \dots, w_p be sinks, where p is the smaller number of nodes in the sources or sinks. Moreover, there exists at least one path p_i from s_i to w_i for $1 \leq i \leq p$. We add edges along the reverse path p'_i ($1 \leq i \leq p$) which share the same nodes but have an opposite direction to p_i , if and only if two adjacent nodes on the path p'_i are not connected. For all the nodes except for $s_i, w_i, i = 1, 2, \dots, p$ in G^* , if the node is a source or a sink, we can add a reverse edge to the existing edge. If the node is an isolated node, we find the node nearest to it, and add two edges, which have reverse directions with each other. Now that we have added edges to G^* , we transfer from adding the edges between two SCCs in G^* to adding the edges between two nodes in G , and then add the edges directly (Fig. 1E).

3. Information transfer on the graph

Information propagates along the strongly connected graph, and each bird in the flock can perceive information from its neighbors. We use matrix A with entries 0 and 1 to represent the connection between birds, where $A_{ij} = 1$ means that bird i can perceive information from bird j , and vice versa. Birds spend a response time τ to sense information. In order to simulate this phenomenon, we use the accumulated time to count the time elapsed in a response period. We first set the response time τ as a constant. The accumulated time \mathbf{T}_{j+1} of all birds at the frame $j + 1$ is generated from $\mathbf{T}_j = (T_{j,1}, T_{j,2}, \dots, T_{j,N})^T$, $\tau > T_{j,i} \geq 0$, and $T_{j+1,i} = H(\tau - T_{j,i} - \Delta t)(T_{j,i} + \Delta t)$, where the Heaviside function $H(x) = 0$ for $x < 0$ and 1 otherwise. As a result,

$$\mathbf{T}_{j+1} = \text{diag}(H(\mathbf{1}\tau - \mathbf{T}_j - \mathbf{1}\Delta t))(\mathbf{T}_j + \mathbf{1}\Delta t), \quad (1)$$

where Δt is the time unit, $\text{diag}(\mathbf{X})$ indicates where the main diagonal equals to the vector \mathbf{X} , and $\mathbf{1} = (1, 1, \dots, 1)^T$.

The state of an external stimulus that affects the behavior of the flock may change over time. We use $s_j \in \mathbb{N}$ to represent ID for the state of the external stimulus at frame j , where $s_{j+1} = s_j + 1$, and $s_0 = 1$. Due to the delay of information transfer, the state of the external stimulus perceived by each bird may be different at the same time. We use the vector $\mathbf{S}_j = (S_{j,1}, S_{j,2}, \dots, S_{j,N})^T$ to represent the information state IDs of the external stimulus of the flock that birds perceive at frame j . Each bird in the flock senses the external information from its neighbors at every τ time. It updates its current information state according to the newest information. The information state \mathbf{S}_{j+1} at frame $j + 1$ can be updated from \mathbf{T}_j and \mathbf{S}_j (Eq. 2).

$$\mathbf{S}_{j+1} = \text{diag}(H(\mathbf{T}_j + 1\Delta t - \tau))(B_1, \dots, B_i, \dots, B_N)^T, \quad (2)$$

where $B_i = \|\text{diag}(\mathbf{A}_i)\mathbf{S}_j\|_\infty$, and \mathbf{A}_i is the i th row of \mathbf{A} , and the initial state of $\mathbf{S}_0 = (0, 0, \dots, 0)^T$. When an external stimulus appears around the flock, n_r birds that are nearest to this stimulus will perceive it first. For simplification, we call n_r a reaction number. The information state \mathbf{S}_j corresponding to these n_r birds will be s_j , accordingly.

3.1. Information transfer time

We define the longest directed path starting from one of the n_r birds for information propagation as l . The information transfer time Q refers to the time when $S_{j,i} \neq 0$, for all $i = 1, 2, \dots, N$, and

$$Q = l\tau. \quad (3)$$

For simulation, the information transfer time could be

$$T = l \left\lceil \frac{\tau}{\Delta t} \right\rceil \Delta t, \quad (4)$$

where $\tau \geq \Delta t$.

According to Eqs. (1) to (4), we choose the number of birds N , the response time of birds τ , the reaction number n_r , and the time unit Δt as the main influencing factors for the information transfer time Q of the flock. The simulation results are shown in Fig. 2.

The information transfer simulation time T grows logarithmically with the number of birds N in the flock (Fig. 2A). Because information transfers through the graph with linear speed, the number of nodes perceiving the information increases exponentially. As a result, the depth of information transfer in the graph is linearly related to $\log(N)$. In other words, $l \propto \log(N)$, and thus $Q \propto \log(N)$ according to Eq. 3. The information transfer simulation time T is proportional to the response time τ (Fig. 2B). This simulation result agrees with Eq. 3, which shows $Q \propto \tau$.

The information transfer simulation time T is inversely proportional to the number of reaction birds n_r , but the decline of T is only approximately 3.7% from 6 to 78 reaction

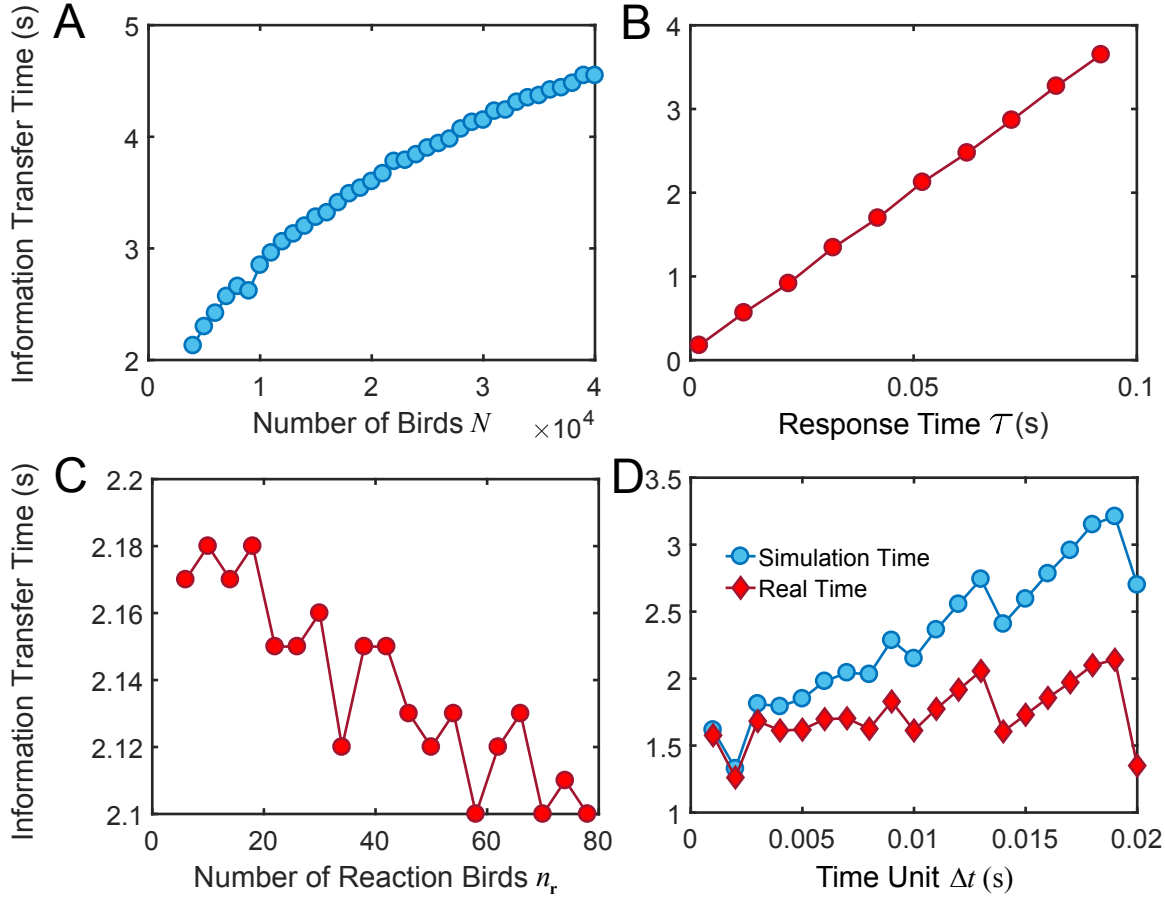


Figure 2. The analysis of information transfer time. (A) The information transfer time with different numbers of birds in one flock with the number of birds n ranging from 4,000 to 40,000, response time $\tau = 0.04\text{s}$, reaction number $n_r = 40$, and time unit $\Delta t = 0.01\text{s}$. (B) The information transfer time with different response times τ of birds, $N = 4,000$, $n_r = 40$, and $\Delta t = 0.01\text{s}$. (C) The information transfer time with different numbers of reaction birds, $\tau = 0.04\text{s}$, $N = 4,000$, and $\Delta t = 0.01\text{s}$. (D) The information transfer time with different time units, $\tau = 0.04\text{s}$, $n_r = 40$, and $N = 4,000$. The blue curve represents the information transfer time in the simulation, and the red curve represents the estimation of real information transfer time in which the simulation error is eliminated.

birds, according to Fig. 2C. To estimate the theoretical time saved with an arbitrary n_r compared to $n_r = 1$, we can compute the information transfer time from 1 bird to n_r birds. Ideally, the information transfer time is $Q = \log_6(\frac{N}{n_r})\tau$. Thus the transfer time saved with 78 birds compared to six birds could be 0.036s ($\tau = 0.04\text{s}$, ‘6’ is the ideal number of neighbors for each bird). The fluctuation of Q in Fig. 2C mainly results from the randomness of the structure of graph G in each simulation.

The information transfer simulation time T is proportional to Δt according to Fig. 2D. However, Q should be irrelevant to Δt according to Eq. 3 given that Q is only relevant to l and τ . This may result from the simulation error e . According to Eq. 4, the range of error e could be $e \in [0, l\Delta t]$. We set $e = l\Delta t$ and obtain an estimate of the information transfer time, $\tilde{T} = T - l\Delta t$. As shown in Fig. 2D, the estimation of \tilde{T} is

irrelevant to Δt , and this result is consistent with Eq. 3.

3.2. The process of information transfer through the flock

We simulate information propagation through the bird flocks and rank all birds in the flock according to the moment when they first become aware of the external stimulus. To verify the accuracy of our method, we also compare our results with the empirical observations from Attanasi et al. [36].

Until now, we have discussed information transfer time with the hypothesis that the response time of birds is constant. In the real world, however, the response time cannot be exactly the same for all birds, even for birds under the same physical conditions. We compare the ranking orders during an information transfer process in which τ is a constant and obeys a Gaussian distribution, which results in $\tau \sim N(\mu, \sigma^2)$. We set a minimum value for τ with Gaussian distribution because τ cannot be a negative value.

If τ is a constant, there are more birds perceiving the external information at the same time, while the ranking curve is more continuous with τ being a Gaussian distribution (Fig. 3A). We find that the ranking curve of the flock with τ obeying a Gaussian distribution is closer to the real world, according to the empirical observations.

The information transfer network with a stable connection is easy to control; we only need to set parameters of the distribution of τ , including means μ , standard deviations σ , and minimum values to generate various results (Fig. 3B). Meanwhile, our model captures the characteristics of the ranking of birds in a flock according to the results, and they are consistent with the empirical observations.

We also test our method with different sizes of flocks as shown in Fig. 3C and D in small flocks and large flocks, respectively. Further, these ranking curves are similar in shape, which indicates that the number of birds that sense the information increases slowly, then rapidly, and finally slowly again. The number of birds that perceived information $n(t)$ increases exponentially at first, which meets the ideal estimation that $n(t) = n_r 6^{\frac{t}{\tau}}$. Because of the fixed flock size N in one simulation, the change of $n(t)$ is finally decreased.

4. Stable information transfer network vs. unstable information transfer network

Traditional methods assume that individuals interact with nearest individuals within a certain Euclidean distance [22, 37, 38]. Recently, scientists discovered that a bird interacts with six to seven birds on average [31, 5]. Combining these advanced works, we compare our stable information transfer network with an unstable information transfer network in which each bird considers the six nearest birds. The stable information transfer network is static, while the unstable one is temporal. In this section, we compare the properties of these two networks.

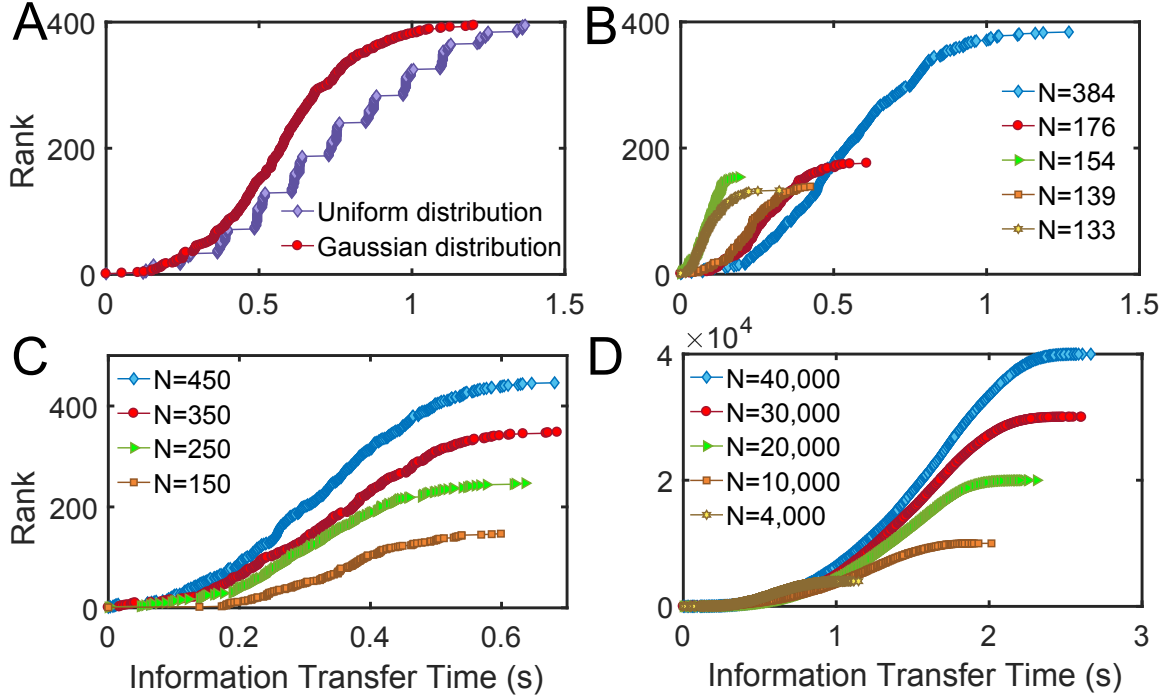


Figure 3. The process of information transfer through the flock described by the ranking curve of birds according to the time when they perceive information. (A) Comparison with different generation methods of response time τ for birds: constant (the purple curve) and Gaussian distribution (the red curve) of different birds. τ is invariant for one bird with a Gaussian distribution. (B) Simulation results with different sizes of flocks for comparison with real datasets [36]. (C) Simulation results with a small number of birds in one flock; the number of birds ranges from 150 to 450. They share the same value of parameters: the distribution of τ , the reaction number of birds n_r , and the time unit Δt . (D) Simulation results with a large number of birds in one flock, with the number of birds ranging from 4,000 to 4,0000. They also share the same parameters.

4.1. Self-propelled model

Grouping individuals adjust their velocities according to those of their local neighbors and external stimuli. In existing particle-based models [22, 30, 37], local interactions occur only among nearest individuals. Instead, we believe that individuals in a group mainly have local interactions with fixed sets of individuals. We use cohesion force, alignment force and repulsion force to describe the effects of local interactions among birds based on the interaction rules in Ref. [37] (see *Appendix A* for more details). In distinction from the existing particle-based models, cohesion force and alignment force only occur among individuals that have connections with each other, while repulsion force occurs among individuals within a certain distance for collision avoidance.

With this self-propelled model, we can simulate bird flocks avoiding a predator, which is a common behavior for bird flocks. By analyzing ranking curve, polarization $\Phi_j = \left\| \frac{1}{N} \sum_{i=1}^N \frac{v_{i,j}}{\|v_{i,j}\|} \right\|$ (which measures the overall degree of alignment), and spatial correlations ($C(r)$ measures behavior correlation among birds with distance $d \in$

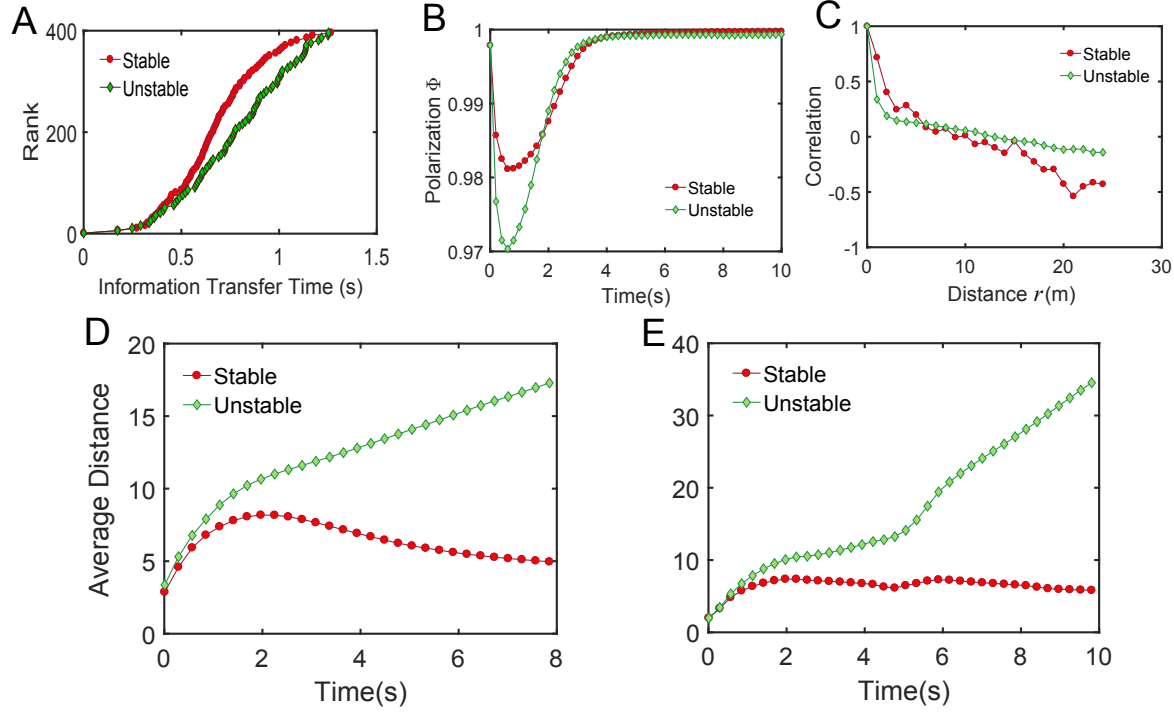


Figure 4. Comparison between the stable information transfer network (the red curve) and the unstable one (the green curve). (A) The rank of each bird in an information transfer sequence is plotted versus the time when it perceives the information. (B) Polarization as a function of time in stable or unstable information transfer networks. (C) This correlation function measures correlation to the extent of the orientation of velocity fluctuations. It is the average inner production of the velocity fluctuations of bird pairs at a mutual distance r . (D) The average distance is plotted versus the time with a fixed external stimulus (predator) attacking the bird flock. (E) The average distance is plotted versus the time with a moving external stimulus (predator) attacking the bird flock.

$[r-1, r]$), we compare stable information transfer networks and unstable information transfer networks with the empirical observations [36, 35].

The ranking curve of the stable information transfer network is an S-curve, while that of an unstable information transfer network is an exponential curve (Fig. 4A). This is because, for an unstable information transfer network, a bird will move towards the flock once it senses danger and transfer that information to birds that are far from it. The ranking curve for the stable information transfer network is closer to that of the empirical observation [36].

Polarization is a quantity that describes the coherence of the flock. If $\Phi_j = 0$, the directions taken by the birds in this flock are totally random, while if $\Phi_j = 1$, all birds in this flock have the same direction. The polarization for a stable information transfer network is larger than that for an unstable information transfer network (Fig. 4B). This shows that the behaviors of birds in the flock with a stable information transfer network are more consistent when they confront a predator.

The spatial correlation of fluctuation (see *Appendix B* for details) is plotted in

Fig. 4C. The spatial correlation of the flock with a stable information transfer network is close to 1 at short distances, decays dramatically with a gradually decreasing rate as the distance increases, and tends to be negative at large distances. Although the spatial correlation with an unstable information transfer network decays dramatically at short distances, it decays with an approximately constant rate as distance increases. The spatial correlation for a stable information transfer network is closer to the real-world one [35].

We use average distance between each bird and the center of the flock D_j to describe the degree of cohesion of the flock at frame j ,

$$D_j = \frac{1}{N} \sum_{k=1}^N \left\| \mathbf{P}_{j,k} - \frac{1}{N} \sum_{i=1}^N \mathbf{P}_{j,i} \right\|_2,$$

where $\mathbf{P}_{j,k}$ and $\mathbf{P}_{j,i}$ are the position of bird k and bird i , respectively. We compare the cohesion degree between the stable information transfer network and the unstable one, and the results are illustrated in Fig. 4D-E. The flock simulated by our method can maintain cohesion as time passes, while the flock simulated by the method with unstable information transfer network cannot maintain cohesion, and birds become far away from each other gradually (see Movie S3-S4).

We compare simulation results of the stable information network with that of the unstable information transfer network visually (see Movie S1-S2). We test these two methods with a fixed danger stimulus and a moving danger stimulus separately. Birds simulated by our method can keep cohesion over time, while birds fly separately with the unstable information transfer network.

5. Discussion and conclusions

To summarize, our information transfer network model depicts how bird flocks perceive and respond to external stimuli. Based on this information transfer network, we consider another type of interactions among individuals by suggesting that an individual does not always interact with its nearest neighbors, but instead interacts with a fixed set of birds in a limited time.

For a long period, people believed that animals can be influenced by neighbors within a certain distance. Recently, researchers have claimed that the interactions between birds in a flock depend on topological distance, rather than metric distance [31, 5]. The neighborhood of each bird is still governed by distance, and there are usually a fixed number of nearest neighbors [30]. Particle-based approaches [22, 30, 39, 40] have been proposed to describe the mechanical dynamics of individuals. In our case, the neighborhood of each bird is static; birds therefore mainly communicate with a fixed set of birds in their neighborhood. Combined with a self-propelled model of birds in a flock, we explore the properties of locomotion with a stable information transfer network or with an unstable one. We find that with a stable information transfer network, the experiment results are robust and closer to both the statistical results generated from

empirical datasets [35, 36] and the empirical observations (Movie S3-S4).

Simulating the information transfer process with a stable network, we find that the information transfer time increases logarithmically with the increase of the flock's size and linearly with the growth of the response time. These results are consistent with the theoretical conclusion drawn from Eq. 4. The number of birds reacting to an external stimulus will affect the total information transfer time of the flock, but the effect is negligible. The method with the response time that obeys a Gaussian distribution generates results closer to the empirical datasets, because the real response time of birds can vary due to position difference, orientation difference, body conditions, etc.

One possible reason for the superiority of stable information network can be that birds are social animals, and they tend to fly with the birds that have social relationships with them [41, 42, 43]. We set the social strength of birds as six, according to the finding that each bird communicates with six to seven neighbors on average [31]. In the real world, the size of different social pairs might vary, while more experimental datasets are needed for further validation of the information transfer network. We also simplify the external stimuli in simulations, although flocks might experience different stimuli at the same time in real-world scenarios. Further investigations are needed on how flocks balance these dangers or attractions.

In addition to the dynamics of bird flocks, our approach can be applied to other related fields. The stable information transfer network is general and applicable to investigate collective behaviors of other social animals. Our method can also be extended to construct the communication networks of unmanned aerial vehicle groups, robotics, and any other self-organized intelligent agent groups [44, 45, 46]. Moreover, The stable information transfer network can also be extended to the temporal scenario in which individuals might change their interaction relationships at heterogeneous time scales [47, 48, 49].

Acknowledgments

Xiaogang Jin was supported by the National Key R&D Program of China (Grant no. 2017YFB1002600). Dinesh Manocha is supported in part by ARO Contract W911NF-10-1-0506 and the National Thousand Talents Program of China. Aming Li acknowledges the generous support from the Chair of Systems Design at ETH Zurich.

Appendix A. Self-propelled model

Grouping individuals adjust their velocity according to that of their neighbors and external stimuli (see Eq. 5). We use mechanical force to represent the factors that drive an individual,

$$\mathbf{F}_{j,i} = \mathbf{F}_{j,i}^{\text{inter}} + \mathbf{F}_{j,i}^{\text{sti}}, \quad (5)$$

where $\mathbf{F}_{j,i}$ is the force works on individual i at frame j , $\mathbf{F}_{j,i}^{\text{inter}}$ is force about interactions with other birds, and $\mathbf{F}_{j,i}^{\text{sti}}$ is the stimulus force when individual i perceives the

information about external stimuli.

The velocity of each individual can be computed according to the following equation,

$$m \frac{\Delta \mathbf{v}_{j,i}}{\Delta t} = \mathbf{F}_{j,i}, \quad (6)$$

where m is the mass of one individual, $\mathbf{v}_{j,i}$ is the velocity of individual i at frame j , and $\Delta \mathbf{v}_{j,i}$ is the difference of $\mathbf{v}_{j,i}$.

Interaction force $\mathbf{F}_{j,i}$ consists of three parts: long-range cohesion $\mathbf{F}_{j,i}^{\text{coh}}$, intermediate-range alignment $\mathbf{F}_{j,i}^{\text{ali}}$ and short-range repulsion $\mathbf{F}_{j,i}^{\text{rep}}$,

$$\mathbf{F}_{j,i}^{\text{inter}} = \mathbf{F}_{j,i}^{\text{coh}} + \mathbf{F}_{j,i}^{\text{ali}} + \mathbf{F}_{j,i}^{\text{rep}}. \quad (7)$$

Cohesion force $\mathbf{F}_{j,i}^{\text{coh}}$ and alignment force $\mathbf{F}_{j,i}^{\text{ali}}$ only occur among individuals that have social relationships with each other, while repulsion force $\mathbf{F}_{j,i}^{\text{rep}}$ occurs among individuals within a certain distance for collision avoidance. We compute $\mathbf{F}_{j,i}^{\text{inter}}$ from two views, graph view for cohesion force $\mathbf{F}_{j,i}^{\text{coh}}$ and alignment force $\mathbf{F}_{j,i}^{\text{ali}}$ (Fig. 5A), and grid view for repulsion force $\mathbf{F}_{j,i}^{\text{rep}}$ (Fig. 5B).

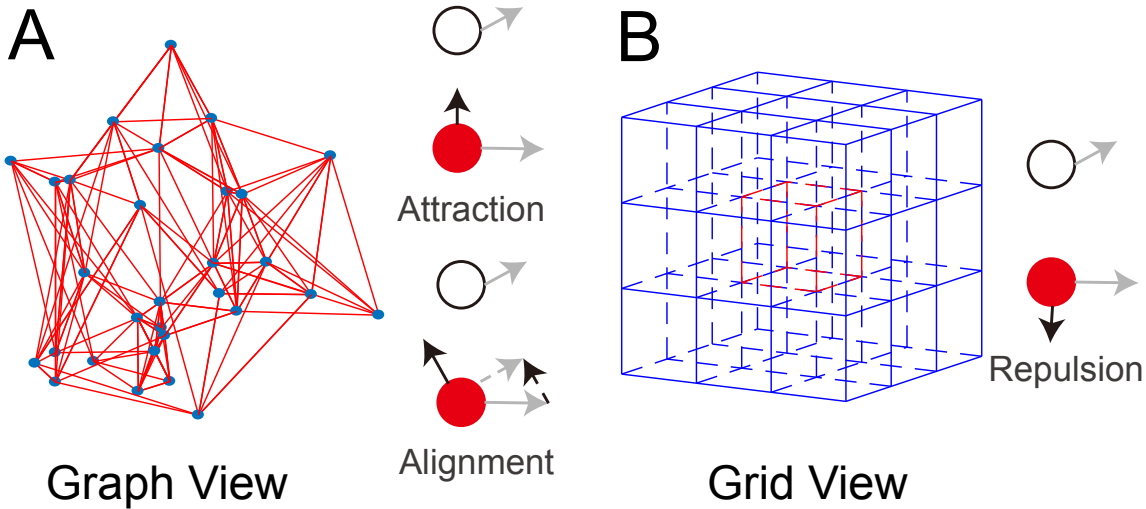


Figure 5. Graph view and grid view. The red nodes refer to the birds that we focus on, the white nodes refer to the birds around them, the grey arrows refer to the directions of birds, and the black arrows refer to the directions of forces, respectively. (A) Graph view. The 3D graph represents the stable information transfer network. The blue nodes refer to the birds, and the red lines refer to the social relationships between birds. Attraction and alignment mainly occur between birds that have connections in the graph. (B) Grid view. The 3D grids are segmentations of the 3D space in which the bird flock flies. The red cube represents the minimal sub-grid to which the bird that we focus on belongs. Repulsion occurs among birds in the same or adjacent minimal sub-grid.

Graph View: In graph view, we treat the flock as an invariant directed graph (Fig. 5A), which represents the stable information transfer network, and use it to compute the attraction force and alignment force. The borders of zones for repulsion, alignment, and attraction for a given bird are defined by the radii d_r and d_c with

$d_c \geq d_r \geq 0$. An individual attempts to keep cohesion with its neighbors within the zone of cohesion. The cohesion force is defined as

$$\mathbf{F}_{j,i}^{\text{coh}} = \frac{w_{\text{coh}}}{n_{j,i}^{\text{coh}}} \sum_{k \in N_i^{\text{coh}}} \frac{\mathbf{P}_{j,k} - \mathbf{P}_{j,i}}{\|\mathbf{P}_{j,k} - \mathbf{P}_{j,i}\|_2}, \quad (8)$$

where $\mathbf{P}_{j,k}$ and $\mathbf{P}_{j,i}$ are the position of bird k and bird i , respectively, and w_{coh} is the weight of $\mathbf{F}_{j,i}^{\text{coh}}$. $N_i^{\text{coh}} = \{k | k \in N_i, \|\mathbf{P}_{j,i} - \mathbf{P}_{j,k}\|_2 \geq d_c\}$ is the set of neighbors of bird i that are in the scope of cohesion, and $n_{j,i}^{\text{coh}}$ is the number of birds in N_i^{coh} .

An individual attempts to keep alignment with its neighbors within the zone of alignment. The alignment force is defined as

$$\mathbf{F}_{j,i}^{\text{ali}} = \frac{w_{\text{ali}}}{n_{j,i}^{\text{ali}}} \sum_{k \in N_i^{\text{ali}}} \frac{\mathbf{v}_{j,k} - \mathbf{v}_{j,i}}{\|\mathbf{v}_{j,k} - \mathbf{v}_{j,i}\|_2} \quad (9)$$

where w_{ali} is the weight of $\mathbf{F}_{j,i}^{\text{ali}}$, $N_i^{\text{ali}} = \{k | k \in N_i, d_c > \|\mathbf{P}_{j,i} - \mathbf{P}_{j,k}\|_2 \geq d_r\}$ is the set of neighbors of bird i that are in the scope of alignment, and $n_{j,i}^{\text{ali}}$ is the number of birds in N_i^{ali} .

Grid View: In grid view, we treat the space in which the bird flock flies as a 3D moving grid (Fig. 5B). We use this 3D moving grid to compute the repulsion force.

An individual attempts to keep repulsion with its neighbors within the zone of repulsion. The repulsion force is defined as

$$\mathbf{F}_{j,i}^{\text{rep}} = \frac{w_{\text{rep}}}{n_{j,i}^{\text{rep}}} \sum_{k \in N_i^{\text{rep}}} \frac{\mathbf{P}_{j,i} - \mathbf{P}_{j,k}}{\|\mathbf{P}_{j,i} - \mathbf{P}_{j,k}\|_2} \quad (10)$$

where w_{rep} is the weight of $\mathbf{F}_{j,i}^{\text{rep}}$, $N_i^{\text{rep}} = \{k | \|\mathbf{P}_{j,i} - \mathbf{P}_{j,k}\|_2 \leq d_r\}$ is the set of neighbors of bird i that are in the scope of repulsion, and $n_{j,i}^{\text{rep}}$ is the number of birds in N_i^{rep} .

In order to search neighbors efficiently, we construct a hash table (Fig. 6 C) by splitting the space around the flock into small grids (Fig. 6 A). The center of the 3D grids is the center of the bird flock. The hash table represents the data structure storing the information about which grid one bird belongs to. Each data element in the hash table corresponds to a grid in 3D storing all IDs of birds that belong to this grid. When we compute the repulsion force for one bird, we only need to search the grid that this bird belongs to and the grids that are adjacent to this grid. With the hash table, the time complexity for searching birds becomes $O(N)$ rather than $O(N^2)$.

Stimulus Force When individuals perceive information about a predator, they try to run away from it. We define the stimulus force as

$$\mathbf{F}_{j,i}^{\text{sti}} = \frac{\mathbf{P}_{j,i} - \mathbf{P}_j^{\text{pre}}}{\|\mathbf{P}_{j,i} - \mathbf{P}_j^{\text{pre}}\|_2}, \quad (11)$$

where $\mathbf{P}_j^{\text{pre}}$ is the position of the predator at frame j .

Then the stimulus force for attraction could be:

$$\mathbf{F}_{j,i}^{\text{sti}} = \frac{\mathbf{P}_j^{\text{att}} - \mathbf{P}_{j,i}}{\|\mathbf{P}_j^{\text{att}} - \mathbf{P}_{j,i}\|_2}, \quad (12)$$

where $\mathbf{P}_j^{\text{att}}$ is the position of the attraction at frame j .

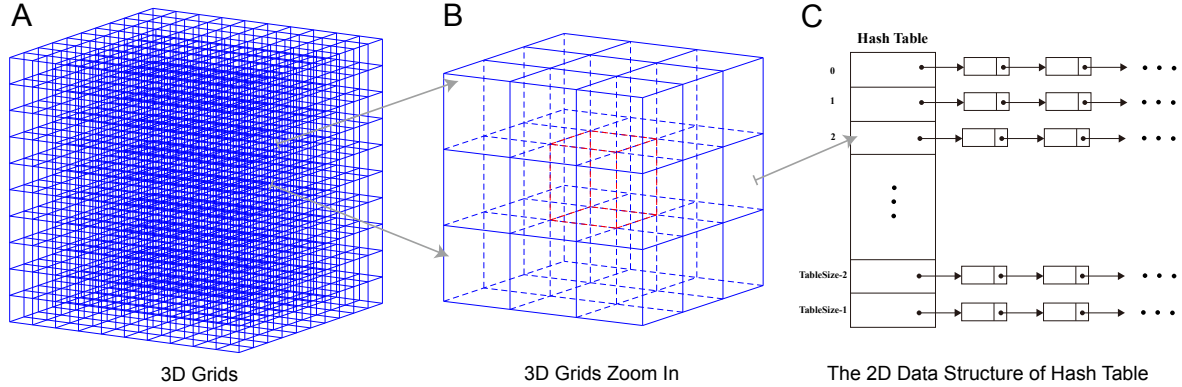


Figure 6. 3D grids and hash table. (A) 3D grids split the flying space of bird flock. (B) Twenty seven grids are zoomed in. (C) The hash table is the data structure storing the information about the grid to which each bird belongs. The size of the hash table equals the number of the 3D grids. Each element of the hash table corresponds to a grid in (A) storing the IDs of birds that belong to this grid.

If there are more than one external stimuli, the stimulus force will be:

$$\mathbf{F}_{j,i}^{\text{sti}} = \frac{1}{N_s} \sum_{k=1}^{N_s} \frac{\mathbf{P}_j^{\chi_k} - \mathbf{P}_{j,i}}{\|\mathbf{P}_j^{\chi_k} - \mathbf{P}_{j,i}\|_2}, \quad (13)$$

where N_s is the number of external stimuli, $\chi_k \in \{\text{pre, att}\}$.

Appendix B. Construction of strongly connected graph

The algorithm about how to construct a strongly connected graph is interpreted as algorithm 1. Taking the set of nodes V as input, we first add edges e_{ji} for each node i with their six nearest neighbors $j \in \Omega_i$, and then add edges to make G strongly connected.

To simplify the graph G , we use the well-known Tarjan's algorithm [50] to find strongly connected components (**SCCs**) for G , and condensing G into a directed acyclic graph G^* , thus obtain sources (with indegree zero), sinks (with outdegree zero), and isolated nodes (with both indegree and outdegree zero) of G^* . The nodes of G^* correspond to the strongly connected components of G . This step corresponds to the function **findSCC** in algorithm 1.

Let s_1, s_2, \dots, s_p be sources in G^* , and w_1, w_2, \dots, w_p be sinks, where p is the smaller number of nodes in the sources or sinks. Moreover, there exists at least one path p_i from s_i to w_i for $1 \leq i \leq p$. We add edges along the reverse path p'_i ($1 \leq i \leq p$) which share the same nodes but have an opposite direction to p_i , if and only if two adjacent nodes on the path p'_i are not connected. For all the nodes except for $s_i, w_i, i = 1, 2, \dots, p$ in G^* , if the node is a source or a sink, we can add a reverse edge to the existing edge. If the node is an isolated node, we find the node nearest to it, and add two edges, which have reverse directions with each other. This step corresponds to the function

addEdges2SCC in algorithm 1.

Now that we have added edges to G^* , we transfer from adding the edges between two SCCs in G^* to adding the edges between two nodes in G , and then add the edges directly. This step corresponds to the function **addEdges2Graph** in algorithm 1.

5.1. Spatial Correlation

Spatial correlation quantifies the behavior correlation among birds in a certain range of distance [35]. Its definition is

$$C(r) = \frac{1}{c_0} \frac{\sum_{ik} \mathbf{u}_i \cdot \mathbf{u}_k H(r - r_{ik}) H(r_{ik} - r + 1)}{\sum_{ik} H(r - r_{ik}) H(r_{ik} - r + 1)},$$

where r_{ik} is the distance between bird i and j , and c_0 is a normalization factor such that $C(r=0) = 1$. \mathbf{u}_i is the fluctuation of bird i around the mean velocity of the flock,

$$\mathbf{u}_i = \mathbf{v}_i - \frac{1}{N} \sum_{k=1}^N \mathbf{v}_k.$$

Algorithm 1:

Algorithm for Constructing a Strongly Connected Graph

Input : the set of nodes V in the Graph G .

Output: Strongly Connected Graph G

Initialization:

Add edges for each node v in G to their six nearest neighbors.

$G' \leftarrow G$; $groupNum \leftarrow NodesNum$

while $groupNum > 1$ **do**

```

     $[G^*, sccNum] \leftarrow \text{findSCC}(G');$ 
     $[G^*, edgesScc] \leftarrow \text{addEdges2SCC}(G^*);$ 
     $G \leftarrow \text{addEdges2Graph}(edgesScc);$ 
     $G' \leftarrow G^*;$ 
     $gourpNum \leftarrow sccNum;$ 

```

end

Appendix C. Comparison between simulation based on our method and empirical movements of birds

We select two clips of empirical movements of bird flocks (from <https://vimeo.com/121168616> and <https://vimeo.com/121168616> respectively). We design the external stimuli according to the corresponding videos. The comparison results (shown in Movie S3-S4) demonstrate that our method can achieve realistic collective behavior of bird flocks. More simulation results are presented in Movie S5-S6.

Appendix D. SI movies

Movie S1. Visual comparison between the method with a stable information transfer network (our method) and the method with an unstable information transfer network (traditional method). In this case, we test these two methods with a fixed external stimulus (predator).

Movie S2. Visual comparison between the method with a stable information transfer network (our method) and the method with an unstable information transfer network (traditional method). In this case, we test these two methods with a moving external stimulus (predator). Average distance means the average distance between each bird and the center of the flock. Each clip has 400 birds.

Movie S3. Visual comparison between simulation based on our method and empirical movements of birds. In our simulation, we set three stimuli (predator) to control the movements of 10,000 birds.

Movie S4. Visual comparison between simulation based on our method and empirical movements of birds. In our simulation, we set one stimulus (attraction) to control the movements of 10,000 birds.

Movie S5. Photo-realistic rendering of our simulation results. In this simulation, 10,000 birds are attacked by three predators.

Movie S6. Photo-realistic rendering of our simulation results. In this simulation, 10,000 birds are flying led by an external attraction.

References

- [1] Vicsek T and Zafeiris A 2012 *Phys Rep* **517** 71–140
- [2] Sokolov A, Aranson I S, Kessler J O and Goldstein R E 2007 *Phys Rev Lett* **98** 158102
- [3] Kelley D H and Ouellette N T 2013 *Sci Rep* **3**
- [4] Tunstrøm K, Katz Y, Ioannou C C, Huepe C, Lutz M J and Couzin I D 2013 *PLoS Comput Biol* **9** e1002915
- [5] Bialek W, Cavagna A, Giardina I, Mora T, Silvestri E, Viale M and Walczak A M 2012 *Proc Natl Acad Sci USA* **109** 4786–4791
- [6] Moussaïd M, Helbing D and Theraulaz G 2011 *Proc Natl Acad Sci USA* **108** 6884–6888
- [7] Deneubourg J L and Goss S 1989 *Ethol Ecol Evol* **1** 295–311
- [8] Couzin I D and Krause J 2003 *Adv Study Behav* **32** 1–75
- [9] Walker T, Sesko D and Wieman C 1990 *Phys Rev Lett* **64** 408
- [10] Szolnoki A and Perc M 2018 *New Journal of Physics* **20** 013031
- [11] Reynolds C W 1987 *ACM SIGGRAPH Computer Graphics* **21** 25–34
- [12] Kirman A 1993 *Q J Econ* **108** 137–156
- [13] Olfati-Saber R 2006 *IEEE Trans Automat Contr* **51** 401–420
- [14] Xie G and Wang L 2007 *International Journal of Robust and Nonlinear Control* **17** 941–959
- [15] Blumer H 1971 *Soc Probl* **18** 298–306
- [16] Proskurnikov A V, Matveev A S and Cao M 2016 *IEEE Transactions on Automatic Control* **61** 1524–1536
- [17] Shao J, Xie G and Wang L 2007 *IET Control Theory & Applications* **1** 545–552
- [18] Parrish J K and Edelstein-Keshet L 1999 *Science* **284** 99–101
- [19] Lima S L 1993 *The Wilson Bulletin* 1–47
- [20] Seeley T and Morse R 1976 *Insectes Soc* **23** 495–512

- [21] Wu Y, Kaiser A D, Jiang Y and Alber M S 2009 *Proc Natl Acad Sci USA* **106** 1222–1227
- [22] Vicsek T, Czirók A, Ben-Jacob E, Cohen I and Shochet O 1995 *Phys Rev Lett* **75** 1226
- [23] Jadbabai A, Lin J and Morse A S 2003 *IEEE Trans Automat Contr* **48** 988–1001
- [24] Su Q, Li A, Zhou L and Wang L 2016 *New Journal of Physics* **18** 103007
- [25] Su Q, Li A and Wang L 2017 *New Journal of Physics* **19** 103023
- [26] Wang X, Su H, Wang X and Chen G 2016 *Perspectives in Science* **7** 133–139
- [27] Shi H, Wang L, Chu T, Xie G and Xu M 2006 Flocking coordination of multiple interactive dynamical agents with switching topology *Systems, Man and Cybernetics, 2006. SMC'06. IEEE International Conference on* vol 3 (IEEE) pp 2684–2689
- [28] Yu W, Chen G and Cao M 2011 *IEEE Transactions on Automatic Control* **56** 1436–1441
- [29] Nax H H, Perc M, Szolnoki A and Helbing D 2015 *Scientific reports* **5** 12145
- [30] Pearce D J, Miller A M, Rowlands G and Turner M S 2014 *Proc Natl Acad Sci USA* **111** 10422–10426
- [31] Ballerini M, Cabibbo N, Candelier R, Cavagna A, Cisbani E, Giardina I, Lecomte V, Orlandi A, Parisi G, Procaccini A et al. 2008 *Proc Natl Acad Sci USA* **105** 1232–1237
- [32] Zhou B, Tang X and Wang X 2012 Coherent filtering: detecting coherent motions from crowd clutters *Comput Vis ECCV* (Springer) pp 857–871
- [33] Mora T, Walczak A M, Del Castello L, Ginelli F, Melillo S, Parisi L, Viale M, Cavagna A and Giardina I 2016 *Nature Physics* **12** 1153–1157 ISSN 1745-2481
- [34] Eswaran K P and Tarjan R E 1976 *SIAM Journal on Computing* **5** 653–665
- [35] Cavagna A, Cimarelli A, Giardina I, Parisi G, Santagati R, Stefanini F and Viale M 2010 *Proc Natl Acad Sci USA* **107** 11865–11870
- [36] Attanasi A, Cavagna A, Del Castello L, Giardina I, Grigera T S, Jelić A, Melillo S, Parisi L, Pohl O, Shen E et al. 2014 *Nat Phys* **10** 691–696
- [37] Lukeman R, Li Y X and Edelstein-Keshet L 2010 *Proc Natl Acad Sci USA* **107** 12576–12580
- [38] Couzin I D, Krause J, Franks N R and Levin S A 2005 *Nature* **433** 513–516
- [39] Ren J, Wang X, Jin X and Manocha D 2016 *PLoS One* **11** e0155698
- [40] Pearce D J and Turner M S 2015 *J R Soc Interface* **12** 20150520
- [41] Robinson G E, Fernald R D and Clayton D F 2008 *Science* **322** 896–900
- [42] Wilkinson R 1982 *Anim Behav* **30** 1118 – 1128
- [43] Hausberger M, Richard-Yris M A, Henry L, Lepage L and Schmidt I 1995 *Journal of Comparative Psychology* **109** 222
- [44] Anderson B, Cao M, Dasgupta S, Morse A and Yu C 2011 *Communications in Information and Systems* **11** 1–16
- [45] Hâncean M G and Perc M 2016 *Scientific reports* **6** 36152
- [46] Szolnoki A and Perc M 2016 *EPL (Europhysics Letters)* **113** 58004
- [47] Li A, Cornelius S P, Liu Y Y, Wang L and Barabási A L 2017 *Science* **358** 1042–1046
- [48] Holme P and Saramäki J 2012 *Phys Rep* **519** 97–125
- [49] Olfati-Saber R and Murray R M 2004 *IEEE Trans Automat Contr* **49** 1520–1533
- [50] Tarjan R 1972 *SIAM Journal on Computing* **1** 146–160